INTERNATIONAL JOURNAL FOR NUMERICAL METHODS IN FLUIDS, VOL. 14, 1311–1323 (1992)

A MULTIGRID METHOD FOR STEADY INCOMPRESSIBLE NAVIER–STOKES EQUATIONS BASED ON FLUX DIFFERENCE SPLITTING

E. DICK

Department of Machinery, State University of Ghent, Sint Pietersnieuwstraat 41, B-9000 Gent, Belgium

AND

J. LINDEN

Gesellschaft für Mathematik und Datenverarbeitung, F1, D-5205 St. Augustin-Birlinghoven, F.R.G.

SUMMARY

The steady Navier–Stokes equations in primitive variables are discretized in conservative form by a vertex-centred finite volume method. Flux difference splitting is applied to the convective part to obtain an upwind discretization. The diffusive part is discretized in the central way.

In its first-order formulation, flux difference splitting leads to a discretization of so-called vector positive type. This allows the use of classical relaxation methods in collective form. An alternating line Gauss–Seidel relaxation method is chosen here. This relaxation method is used as a smoother in a multigrid method. The components of this multigrid method are: full approximation scheme with F-cycles, bilinear prolongation, full weighting for residual restriction and injection of grid functions.

Higher-order accuracy is achieved by the flux extrapolation method. In this approach the first-order convective fluxes are modified by adding second-order corrections involving flux limiting. Here the simple MinMod limiter is chosen. In the multigrid formulation the second-order discrete system is solved by defect correction.

Computational results are shown for the well known GAMM backward-facing step problem and for a channel with a half-circular obstruction.

KEY WORDS Steady Navier–Stokes equations Flux difference splitting Multigrid methods

INTRODUCTION

Modern upwind discretization methods in compressible flow make use of flux-splitting concepts in flux matrix, flux vector or flux difference form. Currently very popular are the flux-vector-splitting method of Van Leer,[1] the flux-difference-splitting method of Roe[2] and the flux-difference-splitting method of Osher and Chakravarthy.[3] It is not generally recognized that these concepts can also be applied to incompressible flow. Flux-difference-splitting methods for incompressible flow were developed by Hartwich and Hsu[4] and Gorski.[5] These methods, however, use the concept of artificial compressibility in order to construct, through time integration, a solution of the steady incompressible Navier–Stokes equations. Artificial compressibility is, however, not necessary to apply flux-splitting concepts to incompressible flows. This was demonstrated by the first author[6,7] using non-conservative flux matrix splitting. In this paper the flux-difference-splitting concept is used in a similar way in order to come to a conservative discretization. The flux difference splitting is of Roe type.

0271–2091/92/111311–13$06.50

Received February 1991
Revised October 1991

FLUX DIFFERENCE SPLITTING FOR INCOMPRESSIBLE FLOW

The steady Navier–Stokes equations in conservative form for an incompressible fluid are

$$\frac{\partial}{\partial x}u^2+\frac{\partial}{\partial y}uv+\frac{\partial}{\partial x}p=\nu\left(\frac{\partial^2 u}{\partial x^2}+\frac{\partial^2 u}{\partial y^2}\right), \tag{1}$$

$$\frac{\partial}{\partial x}uv+\frac{\partial}{\partial y}v^2+\frac{\partial}{\partial y}p=\nu\left(\frac{\partial^2 v}{\partial x^2}+\frac{\partial^2 v}{\partial y^2}\right), \tag{2}$$

$$c^2\left(\frac{\partial u}{\partial x}+\frac{\partial v}{\partial y}\right)=0, \tag{3}$$

where u and v are the Cartesian components of velocity, c is a constant reference velocity introduced to homogenize the eigenvalues of the system matrices, defined in the sequel, p is the kinematic pressure (pressure divided by density) and ν is the kinematic viscosity coefficient.

The set of equations (1)–(3) can be written in system form as

$$\frac{\partial \mathbf{f}}{\partial x}+\frac{\partial \mathbf{g}}{\partial y}=\frac{\partial \mathbf{f}_v}{\partial x}+\frac{\partial \mathbf{g}_v}{\partial y}, \tag{4}$$

where $\mathbf{f}$ and $\mathbf{g}$ are the convective fluxes and $\mathbf{f}_v$ and $\mathbf{g}_v$ are the viscous fluxes:

$$\mathbf{f}=\begin{pmatrix} u^2+p \\ uv \\ c^2u \end{pmatrix}, \qquad \mathbf{g}=\begin{pmatrix} uv \\ v^2+p \\ c^2v \end{pmatrix}, \qquad \mathbf{f}_v=\begin{pmatrix} \nu(\partial u/\partial x) \\ \nu(\partial v/\partial x) \\ 0 \end{pmatrix}, \qquad \mathbf{g}_v=\begin{pmatrix} \nu(\partial u/\partial y) \\ \nu(\partial v/\partial y) \\ 0 \end{pmatrix}. \tag{5}$$

Differences of the convective fluxes can be written in algebraically exact form as

$$\Delta\mathbf{f}=\begin{pmatrix} 2\bar{u} & 0 & 1 \\ \bar{v} & \bar{u} & 0 \\ c^2 & 0 & 0 \end{pmatrix}\Delta\begin{pmatrix} u \\ v \\ p \end{pmatrix}, \qquad \Delta\mathbf{g}=\begin{pmatrix} \bar{v} & \bar{u} & 0 \\ 0 & 2\bar{v} & 1 \\ 0 & c^2 & 0 \end{pmatrix}\Delta\begin{pmatrix} u \\ v \\ p \end{pmatrix}, \tag{6}$$

where the overbar denotes the algebraic mean of the differenced variables.

The matrices defined by (6) are discrete Jacobians. In the sequel these are denoted by $\mathbf{A}_1$ and $\mathbf{A}_2$. Any linear combination of these Jacobians has the form

$$\mathbf{A}=n_x\mathbf{A}_1+n_y\mathbf{A}_2=\begin{pmatrix} n_x\bar{u}+\bar{w} & n_y\bar{u} & n_x \\ n_x\bar{v} & n_y\bar{v}+\bar{w} & n_y \\ c^2n_x & c^2n_y & 0 \end{pmatrix}, \tag{7}$$

where $\bar{w}=n_x\bar{u}+n_y\bar{v}$. For $n_x^2+n_y^2=1$ the eigenvalues of the Jacobian $\mathbf{A}$ are

$$\lambda_1=\bar{w}, \qquad \lambda_{2,3}=\bar{w}\pm a,$$

with $a=\sqrt{(\bar{w}^2+c^2)}$. The corresponding left and right eigenvector matrices are given by

$$\mathbf{L}=\begin{pmatrix} (\bar{v}\bar{w}+n_yc^2)/a^2 & -(\bar{u}\bar{w}+n_xc^2)/a^2 & (n_x\bar{v}-n_y\bar{u})/a^2 \\ (n_x/2)(\bar{w}/a+1) & (n_y/2)(\bar{w}/a+1) & 1/2a \\ (n_x/2)(\bar{w}/a-1) & (n_y/2)(\bar{w}/a-1) & 1/2a \end{pmatrix}, \tag{8}$$

$$\mathbf{R}=\begin{pmatrix} n_y & (\bar{u}/a)-n_x(\bar{w}/a-1) & (\bar{u}/a)-n_x(\bar{w}/a+1) \\ -n_x & (\bar{v}/a)-n_y(\bar{w}/a-1) & (\bar{v}/a)-n_y(\bar{w}/a+1) \\ 0 & a-\bar{w} & a+\bar{w} \end{pmatrix}, \tag{9}$$

where $\mathbf{R}=\mathbf{L}^{-1}$.

The matrix **A** can be split into positive and negative parts by

$$\mathbf{A}^+ = \mathbf{R}\,\Lambda^+\mathbf{L}, \qquad \mathbf{A}^- = \mathbf{R}\,\Lambda^-\mathbf{L}, \qquad \mathbf{A} = \mathbf{A}^+ + \mathbf{A}^-, \tag{10}$$

where

$$\Lambda^+ = \mathrm{diag}(\lambda_1^+, \lambda_2^+, \lambda_3^+), \qquad \Lambda^- = \mathrm{diag}(\lambda_1^-, \lambda_2^-, \lambda_3^-),$$

with

$$\lambda_i^+ = \max(\lambda_i, 0), \qquad \lambda_i^- = \min(\lambda_i, 0).$$

By positive and negative matrices, matrices with non-negative and non-positive eigenvalues respectively are meant. This allows a splitting of any linear combination of flux differences by

$$\Delta\boldsymbol{\phi} := n_x\Delta\mathbf{f} + n_y\Delta\mathbf{g} = \mathbf{A}^+\Delta\boldsymbol{\xi} + \mathbf{A}^-\Delta\boldsymbol{\xi},$$

where ξ is the vector of dependent variables,

$$\boldsymbol{\xi}^{\mathrm{T}} = \{u, v, p\}.$$

VERTEX-CENTRED FINITE VOLUME FORMULATION

Figure 1 shows the control volume centred around the node (i, j).

The inviscid part of (4) is

$$\frac{\partial \mathbf{f}}{\partial \mathrm{x}} + \frac{\partial \mathbf{g}}{\partial \mathrm{y}} = 0.$$

With piecewise constant interpolation of variables, the flux difference over the surface $S_{i+1/2}$ of the control volume can be written as

$$\Delta\mathbf{F}_{i,i+1} := \mathbf{F}_{i+1} - \mathbf{F}_i = \Delta s_{i+1/2}(n_x\Delta\mathbf{f}_{i,i+1} + n_y\Delta\mathbf{g}_{i,i+1}), \tag{11}$$

where $\Delta s_{i+1/2}$ denotes the length of the surface $S_{i+1/2}$ and n_x and n_y are the components of the unit outward normal.

Using the notation of the previous section, the flux difference is

$$\Delta\mathbf{F}_{i,i+1} = \Delta s_{i+1/2}\mathbf{A}_{i,i+1}\Delta\boldsymbol{\xi}_{i,i+1}. \tag{12}$$

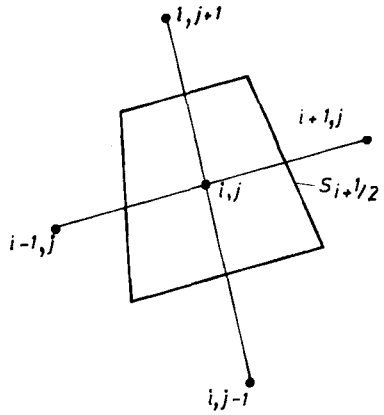

Figure 1. Interior control volume

Furthermore, the matrix $\mathbf{A}_{i,i+1}$ can be split into positive and negative parts. This allows the definition of the absolute value of the flux difference by

$$|\Delta\mathbf{F}_{i,i+1}|=\Delta s_{i+1/2}(\mathbf{A}^{+}_{i,i+1}-\mathbf{A}^{-}_{i,i+1})\Delta\xi_{i,i+1}. \tag{13}$$

Based on (13), an upwind definition of the flux is

$$\mathbf{F}_{i+1/2}=\tfrac{1}{2}(\mathbf{F}_i+\mathbf{F}_{i+1}-|\Delta\mathbf{F}_{i,i+1}|). \tag{14}$$

That this represents an upwind flux can be verified by writing (14) in either of the following two ways, which are completely equivalent:

$$\begin{aligned}\mathbf{F}_{i+1/2}&=\mathbf{F}_i+\tfrac{1}{2}\Delta\mathbf{F}_{i,i+1}-\tfrac{1}{2}|\Delta\mathbf{F}_{i,i+1}|\\&=\mathbf{F}_i+\Delta s_{i+1/2}\mathbf{A}^{-}_{i,i+1}\Delta\xi_{i,i+1},\end{aligned} \tag{15}$$

$$\begin{aligned}\mathbf{F}_{i+1/2}&=\mathbf{F}_{i+1}-\tfrac{1}{2}\Delta F_{i,i+1}-\tfrac{1}{2}|\Delta F_{i,i+1}|\\&=\mathbf{F}_{i+1}-\Delta s_{i+1/2}\mathbf{A}^{+}_{i,i+1}\Delta\xi_{i,i+1}.\end{aligned} \tag{16}$$

Indeed, when $\mathbf{A}_{i,i+1}$ has only positive eigenvalues, the flux $\mathbf{F}_{i+1/2}$ is taken to be $\mathbf{F}_i$, and when $\mathbf{A}_{i,i+1}$ has only negative eigenvalues, the flux $\mathbf{F}_{i+1/2}$ is taken to be $\mathbf{F}_{i+1}$.

The fluxes on the other surfaces of the control volume are treated in a similar way. Using (15) and (16), the inviscid flux balance on the control volume of Figure 1 can be brought into the form

$$\begin{aligned}\Delta s_{i+1/2}\mathbf{A}^{-}_{i,i+1}(\xi_{i+1}-\xi_i)+\Delta s_{i-1/2}\mathbf{A}^{+}_{i,i-1}(\xi_i-\xi_{i-1})+\Delta s_{j+1/2}\mathbf{A}^{-}_{j,j+1}(\xi_{j+1}-\xi_j)\\+\Delta s_{j-1/2}\mathbf{A}^{+}_{j,j-1}(\xi_j-\xi_{j-1})=0.\end{aligned} \tag{17}$$

The set formed by equations (17) for all nodes is so-called positive. The positivity can be seen by writing (17) in the form

$$\begin{aligned}\mathbf{C}\xi_{i,j}=\Delta s_{i-1/2}\mathbf{A}^{+}_{i,i-1}\xi_{i-1,j}+\Delta s_{i+1/2}(-\mathbf{A}^{-}_{i,i+1})\xi_{i+1,j}+\Delta s_{j-1/2}\mathbf{A}^{+}_{j,j-1}\xi_{i,j-1}\\+\Delta s_{j+1/2}(-\mathbf{A}^{-}_{j,j+1})\xi_{i,j+1},\end{aligned} \tag{18}$$

where $\mathbf{C}$ is the sum of the matrices on the right-hand side, all of which have non-negative eigenvalues.

As a consequence of the positivity, a solution can be obtained by a collective variant of any scalar relaxation method. By a collective variant, it is meant that at each node all components of the vector of dependent variables, ξ, are relaxed simultaneously.

In practice, the inviscid flux balance (17) is formed by summing expressions of type (15) over all surfaces using the appropriate components of the unit outward normal, n_x and n_y, in the definition of the Jacobian (7).

In order to define the viscous fluxes $\mathbf{f}_v$ and $\mathbf{g}_v$ in a piecewise constant way on the surfaces of the control volume, approximations to derivatives of u and v are to be calculated at the midpoints of the surfaces. This is done here by the well known Peyret control volume technique. Figure 2 shows the Peyret control volume around the point $(i+\frac{1}{2},j)$.

Integration over the control volume gives

$$\left(\frac{\partial u}{\partial x}\right)_{i+1/2}\Omega_{i+1/2}\approx\int_{\Omega_{i+1/2}}\frac{\partial u}{\partial x}\,\mathrm{d}\Omega=\int_{\Gamma_{i+1/2}}un_x\,\mathrm{d}\Gamma,$$

where $\Gamma_{i+1/2}$ denotes the surface of the control volume. On each side of $\Omega_{i+1/2}$, midpoint rules are used to evaluate the surface integral. Vertex values (at grid points (i,j) and $(i+1,j)$) or mean values over the four surrounding nodes are used.

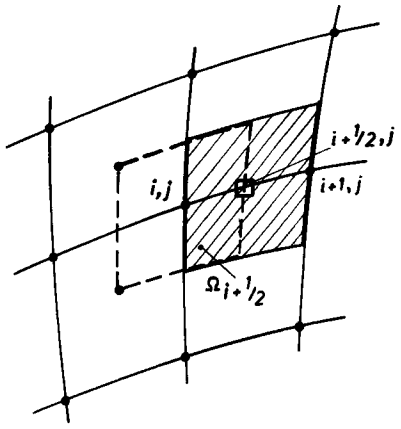

Figure 2. Peyret control volume

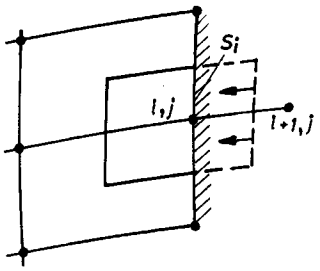

Figure 3. Control volume at a boundary

With the derivatives obtained, the viscous fluxes are calculated at the midpoints of the surfaces of the control volumes around the vertices. The viscous flux balance is then obtained through piecewise constant integration. This results in a central discretization of the viscous flux balance. The structure of the discrete viscous flux balance, when transferred to the left-hand side in (4), is positive in the sense used above. Adding the viscous flux balance to the inviscid flux balance enforces the positivity.

BOUNDARY CONDITIONS

Figure 3 shows the half-volume centred around a node on a boundary. For convenience, the boundary is considered to be an S_i-boundary. This half-volume can be seen as the limit of a complete volume in which one of the sides tends to the boundary.

As a consequence, the convective flux on the side S_i of the boundary control volume can be expressed according to (15) by

$$\mathbf{F}_i + \Delta s_i \mathbf{A}_{i,j}^{-}(\xi_{i+1} - \xi_i), \tag{19}$$

where the matrix $\mathbf{A}_{i,j}$ is calculated at the node (i, j). With the definition (19) the inviscid flux balance on the control volume at the boundary takes the form (17), in which a node outside the domain comes in. This node, however, can be eliminated.

Using the left and right eigenvector matrices (8) and (9), the general expression for $\mathbf{A}^-$ is found to be

$$\mathbf{A}^- = \begin{pmatrix} n_y\bar{w}^-\beta + n_x\lambda^2\hat{u}/2 & -n_y\bar{w}^-\alpha + n_y\lambda^2\hat{u}/2 & (n_y\bar{w}^-\gamma + \lambda\hat{u}/2)/a \\ -n_x\bar{w}^-\beta + n_x\lambda^2\hat{v}/2 & n_x\bar{w}^-\alpha + n_y\lambda^2\hat{v}/2 & (-n_x\bar{w}^-\gamma + \lambda\hat{v}/2)/a \\ -n_x c^2\lambda/2 & -n_y c^2\lambda/2 & -c^2/2a \end{pmatrix}, \tag{20}$$

where

$$\hat{u} = \bar{u} - n_x(\bar{w}+a), \qquad \hat{v} = \bar{v} - n_y(\bar{w}+a), \qquad \lambda = (\bar{w}-a)/a,$$
$$\alpha = (\bar{u}\bar{w} + n_x c^2)/a^2, \qquad \beta = (\bar{v}\bar{w} + n_y c^2)/a^2, \qquad \gamma = (n_x\bar{v} - n_y\bar{u})/a.$$

On a solid boundary, owing to the condition of tangentiality $\bar{w} = n_x\bar{u} + n_y\bar{v} = 0$, expression (20) implifies to (even more simplifications are possible)

$$\mathbf{A}^- = \begin{pmatrix} n_x\lambda^2\hat{u}/2 & n_y\lambda^2\hat{u}/2 & \lambda\hat{u}/2a \\ n_x\lambda^2\hat{v}/2 & n_y\lambda^2\hat{v}/2 & \lambda\hat{v}/2a \\ -n_x c^2\lambda/2 & -n_y c^2\lambda/2 & -c^2/2a \end{pmatrix}. \tag{21}$$

Because rank $(\mathbf{A}^-) = 1$, two independent combinations of the discrete set of inviscid equations exist, eliminating the outside node. These correspond to the first two eigenvectors of $\mathbf{L}$ in (8). The viscous boundary conditions are

$$u = 0, \qquad v = 0. \tag{22}$$

As a consequence, we only need one boundary equation. The first eigenvector in (8) contains the tangential velocity. Existence of tangential velocity at a solid boundary is not consistent with the viscous equations. Therefore the second eigenvector is to be taken. This eigenvector is proportional to

$$(n_x c,\ n_y c,\ 1). \tag{23}$$

This combination is used to determine the pressure at solid walls. The resulting equation is a mass equation corrected with contributions from the momentum equations.

With (23) the viscous terms are combined on the solid boundary in a term proportional to

$$n_x\nabla^2 u + n_y\nabla^2 v = \nabla^2 w.$$

Using the finite volume integration gives

$$\int_\Omega \nabla\cdot(\nabla w)\,\mathrm{d}\Omega = \int_\Gamma \nabla w\cdot\mathbf{n}\,\mathrm{d}\Gamma = \int_\Gamma \frac{\partial w}{\partial n}\,\mathrm{d}\Gamma.$$

On the part of the surface coinciding with the boundary, w stands for the outward normal component of the velocity. Using the mass equation in a co-ordinate system aligned with the boundary gives

$$\frac{\partial w}{\partial n} + \frac{\partial t}{\partial s} = 0,$$

where t is the tangential velocity component and s is the tangential direction. Since obviously $\partial t/\partial s = 0$, the result is

$$\frac{\partial w}{\partial n} = 0.$$

This means that for the viscous terms there is no contribution from the boundary in the combination given by (23).

A similar reasoning applies to the other boundaries.

At outflow, $\bar{w}^- = 0$. This leads also to the simplification of $\mathbf{A}^-$ to the form (21). The combinations eliminating the outside node are again given by the first two eigenvectors of $\mathbf{L}$ in (8). It can immediately be verified in the expression of $\mathbf{A}^-$ given by (21) that these eigenvectors can be combined to give

$$(1, 0, \lambda\hat{u}/c^2), \qquad (0, 1, \lambda\hat{v}/c^2).$$

These determine the u- and v-equations. These equations are momentum equations corrected with a contribution from the mass equation. The boundary condition to be added can be the prescription of pressure ($p = 0$). For fully developed outflow, $\partial u/\partial n = 0$ and $\partial v/\partial n = 0$. Then again there is no contribution in the viscous terms at the boundary.

At inflow, the expression for $\mathbf{A}^-$ given by (20) cannot be simplified. However, the combination (23) still holds. This gives the pressure. Further boundary conditions are prescription of u and v. For fully developed inflow, again there is no contribution in the viscous terms at the boundary.

SECOND-ORDER FORMULATION

Owing to the use of the full upwind discretization for the convective fluxes, only first-order accuracy is obtained up to now. In order to obtain second-order accuracy, the definition of the flux (14) has to be modified.

First we remark that, using (10), the flux difference (12) can be written as

$$\Delta\mathbf{F}_{i,i+1} = \Delta s_{i+1/2} \sum_n \mathbf{r}^n_{i+1/2} \lambda^n_{i+1/2} \mathbf{l}^n_{i+1/2} \Delta\boldsymbol{\xi}_{i,i+1}, \tag{24}$$

where the superscript n refers to the nth eigenvalue and $\mathbf{r}^n$ and $\mathbf{l}^n$ denote the nth right and left eigenvectors.

By denoting the projection of $\Delta\boldsymbol{\xi}_{i,i+1}$ on the nth eigenvector by

$$\sigma^n_{i+1/2} = \mathbf{l}^n_{i+1/2} \Delta\boldsymbol{\xi}_{i,i+1},$$

equation (24) can be written as

$$\Delta\mathbf{F}_{i,i+1} = \sum_n \Delta\mathbf{F}^n_{i,i+1} = \Delta s_{i+1/2} \sum_n \mathbf{r}^n_{i+1/2} \lambda^n_{i+1/2} \sigma^n_{i+1/2} = \Delta s_{i+1/2} \sum_n \mathbf{r}^n_{i+1/2} \tau^n_{i+1/2}, \tag{25}$$

where $\Delta\mathbf{F}^n_{i,i+1}$ is the component of the flux-difference associated with the nth eigenvalue and $\tau^n_{i+1/2}$ is the projection of the flux-difference on the nth eigenvector

Using (25), the first-order flux (14) can be written as

$$\mathbf{F}_{i+1/2} = \tfrac{1}{2}(\mathbf{F}_i + \mathbf{F}_{i+1}) - \tfrac{1}{2} \sum_n \Delta\mathbf{F}^{n+}_{i,i+1} + \tfrac{1}{2} \sum_n \Delta\mathbf{F}^{n-}_{i,i+1}, \tag{26}$$

where the $+$ and $-$ superscripts denote the positive and negative parts of the components of the flux difference, i.e. the parts obtained by taking the positive and negative parts of the eigenvalues.

According to Chakravarthy and Osher,[8] assuming a structured sufficiently smooth grid, a second-order flux corresponding to (26) can be defined by

$$\mathbf{F}_{i+1/2} = \tfrac{1}{2}(\mathbf{F}_i + \mathbf{F}_{i+1}) - \tfrac{1}{2} \sum_n \Delta\mathbf{F}^{n+}_{i,i+1} + \tfrac{1}{2} \sum_n \Delta\mathbf{F}^{n-}_{i,i+1} + \tfrac{1}{2} \sum_n \widetilde{\Delta\mathbf{F}}^{n+}_{i-1,i} - \tfrac{1}{2} \sum_n \widetilde{\Delta\mathbf{F}}^{n-}_{i+1,i+2}, \tag{27}$$

where

$$\widetilde{\Delta \mathbf{F}}^{n+}_{i-1,i} = \Delta s_{i+1/2} \mathbf{r}^n_{i+1/2} \lambda^n_{i+1/2} \mathbf{l}^n_{i+1/2} \Delta \xi_{i-1,i}$$
$$= \Delta s_{i+1/2} \mathbf{r}^n_{i+1/2} \lambda^n_{i+1/2} \tilde{\sigma}^n_{i-1/2}, \tag{28}$$

with a similar definition for $\widetilde{\Delta \mathbf{F}}^{n-}_{i+1,i+2}$.

Clearly, (28) is constructed by considering a flux difference over the surface $S_{i+1/2}$, i.e. using the geometry of this surface, with data shifted in the negative i-direction. $\tilde{\sigma}^n_{i-1/2}$ represents the projection of the shifted difference of the dependent variables on the nth eigenvector of the original flux difference. The second-order correction could also be defined using the τ-variables, i.e. the projections of the flux difference. This would mean that the eigenvalue in (28) is also shifted. In practice, there is little difference between the results of the two formulations. In the sequel we only use (28).

The definition (28) corresponds to a second-order upwind flux. This can be easily seen by considering the case where all eigenvalues have the same sign. Second-order accuracy also can be reached by taking a central definition of the flux vector

$$\bar{\mathbf{F}}_{i+1/2} = \tfrac{1}{2}(\mathbf{F}_i + \mathbf{F}_{i+1}). \tag{29}$$

As is well known, using either (27) or (29) leads to a scheme which is not monotonicity-preserving so that wiggles in the solution become possible. Following the theory of flux limiters,[9] a combination of (27) and (29) is to be taken. This has the form

$$\mathbf{F}_{i+1/2} = \tfrac{1}{2}(\mathbf{F}_i + \mathbf{F}_{i+1}) - \tfrac{1}{2}\sum_n \Delta \mathbf{F}^{n+}_{i,i+1} + \tfrac{1}{2}\sum_n \Delta \mathbf{F}^{n-}_{i,i+1} + \tfrac{1}{2}\sum_n \widetilde{\widetilde{\Delta \mathbf{F}}}^{n+}_{i-1,i} - \tfrac{1}{2}\sum_n \widetilde{\widetilde{\Delta \mathbf{F}}}^{n-}_{i+1,i+2}, \tag{30}$$

with

$$\widetilde{\widetilde{\Delta \mathbf{F}}}^{n+}_{i-1,i} = \mathrm{Lim}(\widetilde{\Delta \mathbf{F}}^{n+}_{i-1,i}, \Delta \mathbf{F}^{n+}_{i,i+1}), \tag{31}$$

$$\widetilde{\widetilde{\Delta \mathbf{F}}}^{n-}_{i+1,i+2} = \mathrm{Lim}(\widetilde{\Delta \mathbf{F}}^{n-}_{i+1,i+2}, \Delta \mathbf{F}^{n-}_{i,i+1}), \tag{32}$$

where Lim denotes some limited combination of both arguments. We choose here the simplest possible form of limiter, i.e. Lim = MinMod, where the function MinMod returns the argument with minimum absolute value if both arguments have the same sign and returns zero otherwise. By the use of the limiter on the vectors (31) and (32) it is meant that the limiter is used per σ-component.

In the vicinity of boundaries, some components of the flux differences in (31) or (32) do not exist. For these components the limiter then returns a zero. This does not degrade the second-order accuracy since, owing to the characteristic boundary treatment, these components do not enter the boundary equations.

The foregoing second-order correction procedure is called the flux extrapolation technique.

MULTIGRID DEFECT CORRECTION FORMULATION

Since for the discretization obtained by the second-order formulation the positivity is not guaranteed, a relaxation solution is impossible. Therefore as solution procedure a defect correction formulation is used. To explain the procedure, we denote symbolically the first and second-order formulations on a grid with mesh size h by

$$L^1_h = r^1_h, \tag{33}$$

$$L^2_h = r^2_h, \tag{34}$$

where L and r indicate left- and right-hand sides respectively.

In a defect correction the following system is constructed:

$$L_h^1 = r_h^1 + [(L_h^1 - r_h^1) - (L_h^2 - r_h^2)]. \tag{35}$$

The term in square brackets is the defect correction. It is the difference between the defects of the first- and second-order discretizations. In our problem the defect is simply the defect of the flux balance. Thus the defect correction is explicitly given by the summation of the flux corrections generated by the flux extrapolation.

In a defect correction procedure an outer iteration is set up in which, in each step, the first-order system is solved (approximately) followed by an update of the defect correction. The steps are repeated up to convergence. Here as solution method for the first-order system a multigrid procedure is used. The multigrid procedure in itself is iterative and serves as an inner iteration. In the examples discussed below, one multigrid cycle is used to obtain an approximate solution of the first-order system. After this cycle the defect correction is updated. Thus the inner and outer iterations are concurrent. After defect correction the inner iteration starts from the current approximation. The multigrid cycle used is the F-cycle and the non-linearity is treated implicitly by the full approximation scheme (FAS). The components of the multigrid cycle are more or less standard: alternating line Gauss–Seidel relaxations in lexicographic order are used for error smoothing where the coefficients of equations (17) are always formed with the latest available information. One alternating sweep is performed before and one after the coarse grid correction step. Within the flow field, restriction of residuals is done by full weighting, while injection is used at the boundaries. Coarse grid corrections are transferred back to finer grids by bilinear interpolation. The FAS restriction of function values is injection.

COMPUTATIONAL EXAMPLES

First, results are presented for the GAMM backward-facing step problem.[10] The grid shown in Figure 4 is the second coarsest in a series of six. We denote this grid by grid 2. The grids are almost rectangular. A grid called grid 4 is twice more refined with respect to the grid shown and has 2834 nodes. We present results on grid 4 and on more refined grids. At inflow, velocity is prescribed (parabolic profile). At outflow, pressure is given. The Reynolds number is 300 based on the maximum inlet velocity and inlet height. The relaxation is organized blockwise. A first block is formed by the nodes upstream of the step (25×17 nodes for grid 4). A second block is formed by the nodes at the step and downstream of the step (73×33 nodes for grid 4). The first block is relaxed first. The calculation starts from zero initial values for all the unknowns on the finest grid. To calculate the solution on grid 4, four grids are used in the multigrid formulation.

Figure 5(a) shows the streamlines obtained on grid 4 after postprocessing for the first-order solution. The first-order solution is obtained by switching off the defect correction. The ratio of the reattachment length to the step height is about 4·6. In comparison with the reference results,[10] this ratio is too short. This is due to the first-order accuracy. Figure 5(b) shows the result obtained on grid 4 with the second-order formulation. Here the reattachment length is 6·4 times the step height. This is about correct for this test case. Figure 5(c) shows the first-order result on a once

Figure 4. Second coarsest grid for the backward-facing step problem

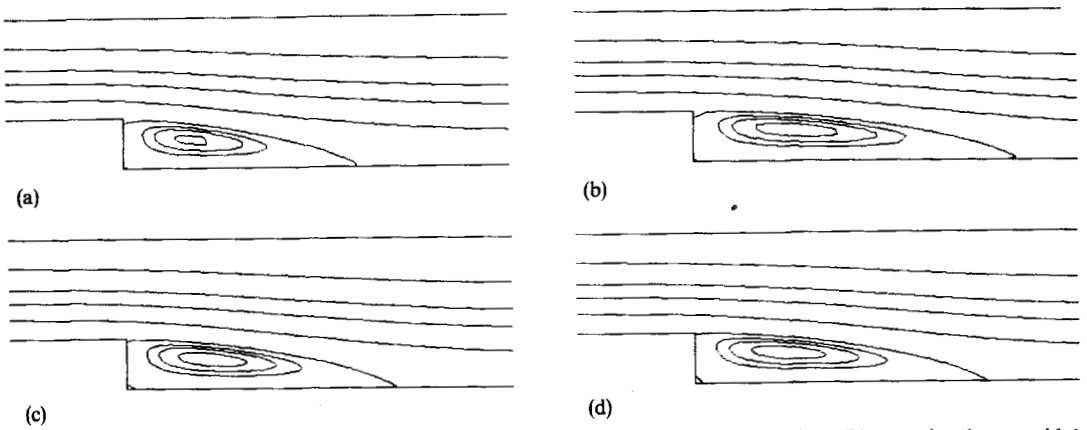

Figure 5. Streamline results for the backward-facing step problem: (a) first-order on grid 4; (b) second-order on grid 4; (c) first-order on grid 5; (d) first-order on grid 6. The streamlines shown are −0·02, −0·015, −0·01, 0, 0·1, 0·3, 0·5 and 0·8

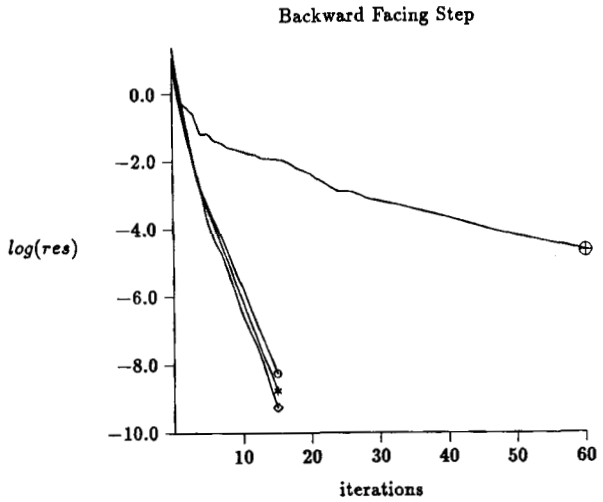

Figure 6. Convergence histories of first-order (◇, grid 4; ○, grid 5; *, grid 6) and second-order (⊕, grid 4) formulations for the backward-facing step problem

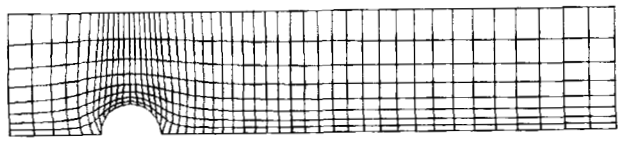

Figure 7. Third coarsest grid for the half-circular obstruction problem

more refined grid (grid 5: 49 × 33 nodes in the first block, 145 × 65 nodes in the second block). Figure 5(d) shows the first-order result on a twice more refined grid (grid 6: 97 × 65 nodes in the first block, 289 × 129 nodes in the second block). The ratio of the reattachment length to the step height is about 5·3 and 5·8 respectively. In comparison with the reference results,[10] this ratio is too short. This shows that the second-order result on the basic grid is of better quality than the first-order results on the refined grids.

Figure 6 shows the convergence behaviour of the solutions shown in Figure 5. The residual is the maximum residual over all equations. Residuals are calculated on the finest grid, based either on the first or second-order flux balance. For the first-order calculation the residuals are taken after the post-relaxation on the finest grid. For the second-order calculation the residuals are taken after the defect correction. By an iteration a basic multigrid cycle is meant. For grid 5 five levels are used in the multigrid cycle and for grid 6 six levels are used. The average convergence

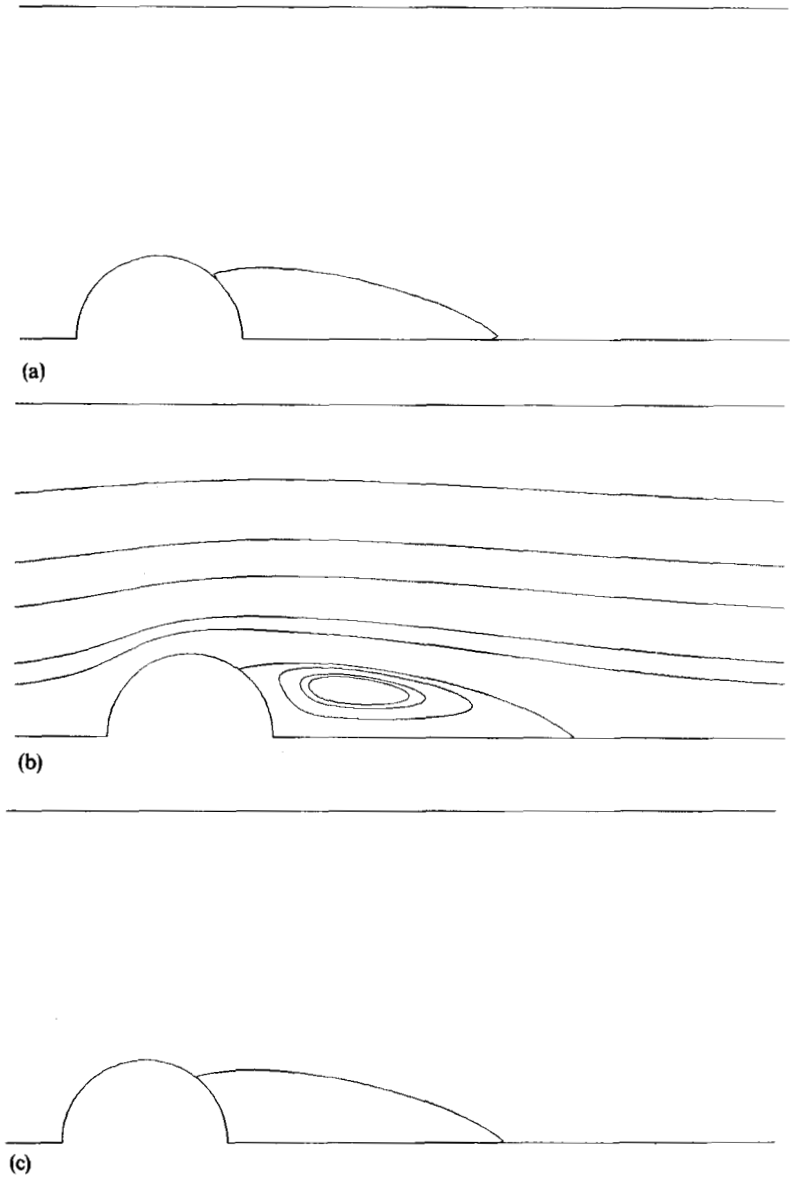

Figure 8. Streamline results for the half-circular obstruction problem: (a) first-order on grid 5; (b) second-order on grid 5; (c) first-order on grid 6; (d) first-order on grid 7. The streamlines shown are −0·007, −0·006, −0·003, 0, 0·05, 0·1, 0·3, 0·5 and 0·8

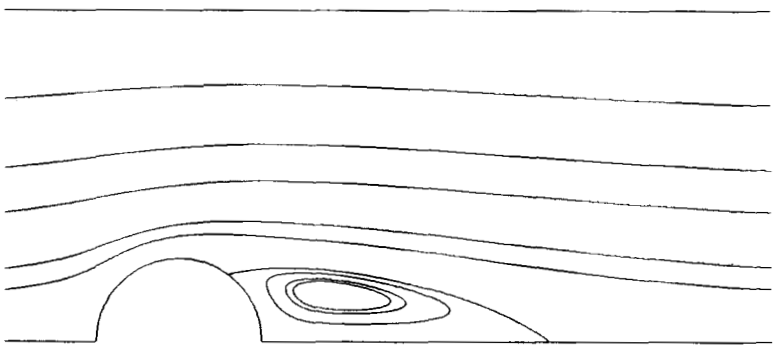

(d)

Figure 8. (Continued)

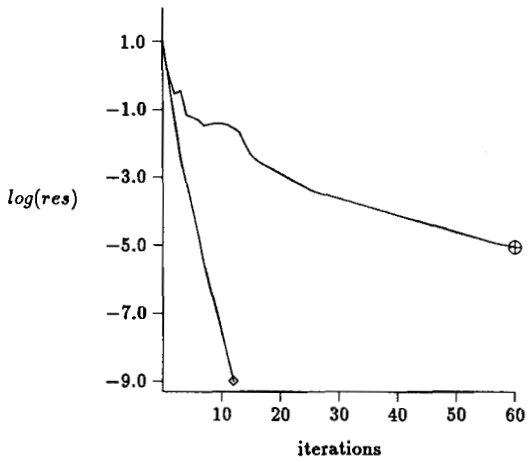

Figure 9. Convergence histories of first-order (◇) and second-order (⊕) formulations on grid 5 for the half-circular obstruction problem

factor per cycle for the first-order solution on grid 4 is about 0·22. The convergence on the other grids is almost identical. This is typical for a basic multigrid method. The average convergence factor per cycle for the second-order solution on grid 4 is about 0·81. The obtained convergence for the second-order solution is not really good. It is, however, comparable to the convergence of similar defect correction procedures for other flow problems, as for instance reported by Koren and Spekreijse[11] for the steady Euler equations. Also for the second-order solutions the convergence deteriorates with the grid refinement (not shown on the figure).

Secondly, results are presented for a channel with a half-circular obstruction as shown in Figure 7. The grid shown has 49×9 nodes. It is the third in a series of seven grids. A twice more refined grid is called grid 5 and has 193×33 nodes. Further refined grids are grid 6 with 385×65 nodes and grid 7 with 769×129 nodes. The flow is calculated for a parabolic inlet velocity profile and for a constant pressure at outlet. The Reynolds number is 100 based on the maximum inflow velocity and diameter of the half-circle.

Figure 8 shows the streamline results for first and second-order solutions on grid 5 and for first-order solutions on grids 6 and 7. The ratio of the reattachment length to the half-circle height is 3·12 for the first-order solution on grid 5. The corresponding ratios for the first-order solutions on grids 6 and 7 are 3·39 and 3·53 respectively. The ratio for the second-order solution is 3·67. This ratio is the same on all grids (second-order solution on grids 6 and 7 not shown). This shows that the second-order solution on grid 5 is already a grid-independent solution. It also shows that the second-order solution is superior to the first-order solution on much finer grids.

Figure 9 shows the convergence behaviour for the first- and second-order formulations for the results on grid 5. Five levels were used in the multigrid method. The average convergence factor per cycle is approximately 0·14 for the first-order solution and 0·79 for the second-order solution. The performance is comparable with the performance for the backward-facing step problem.

CONCLUSIONS

It has been shown that for the steady incompressible Navier–Stokes equations, flux difference splitting can be applied, leading to a set of discrete equations which can be solved by multigrid methods.

The procedure is very similar to the procedure for a compressible fluid but no use of an artificial compressibility is made. The multigrid solution method can be organized in the same way as in compressible flow applications and a comparable multigrid performance is obtained.

REFERENCES

1. B. Van Leer, 'Flux-vector splitting for the Euler equations', *Lecture Notes Phys.*, **170**, 507–512 (1982).
2. P. L. Roe, 'Approximate Riemann solvers, parameter vectors and difference schemes', *J. Comput. Phys.*, **43**, 357–372 (1981).
3. S. Osher and S. R. Chakravarthy, 'Upwind schemes and boundary conditions with applications to Euler equations in general geometries', *J. Comput. Phys.*, **50**, 447–481 (1983).
4. P. M. Hartwich and C. H. Hsu, 'High resolution upwind schemes for the three-dimensional, incompressible Navier–Stokes equations', *AIAA-87-0547*, 1987.
5. J. J. Gorski, 'Solutions of the incompressible Navier–Stokes equations using an upwind-differenced TVD scheme', *Lecture Notes Phys.*, **323**, 278–282 (1989).
6. E. Dick, 'A flux-vector splitting method for steady Navier–Stokes equations', *Int. j. numer. methods fluids*, **8**, 317–326 (1988).
7. E. Dick, 'A multigrid method for steady incompressible Navier–Stokes equations based on partial flux splitting', *Int. j. numer. methods fluids*, **9**, 113–120 (1989).
8. S. R. Chakravarthy and S. Osher, 'A new class of high accuracy TVD schemes for hyperbolic conservation laws', *AIAA-85-0363*, 1985.
9. P. K. Sweby, 'High resolution schemes using flux limiters for hyperbolic conservation laws', *SIAM J. Numer. Anal.*, **21**, 995–1011 (1984).
10. K. Morgan, J. Periaux and F. Thomasset (eds), 'Analysis of laminar flow over a backward facing step', *Notes Numer. Fluid Mech.*, **9**, (1984).
11. B. Koren and S. Spekreijse, 'Solution of the steady Euler equations by a multigrid method', *Lecture Notes Pure Appl. Math.*, **110**, 323–336 (1988).